The BDCE Equivalent Control Method for Multiphase Induction Machine

Nkosinathi Gule (MIEEE) and M. J. Kamper (SMIEEE)

***Abstract*—The concept behind the brush dc equivalent (BDCE) control method for multiphase induction machine is described in this paper. The BDCE concept is developed from the dc machine operation. A method for calculating the air-gap flux density is given in this paper. Calculated and finite element analysis (FEA) evaluated flux density waveforms for a nine-phase induction machine are provided. Also, a comparison of analytically calculated and measured torque of the machine is given.**

I. INTRODUCTION

Generally, the control techniques used in three-phase induction machine drives are modified and developed for the control of multiphase (more than three phases) induction machines. Scalar control with voltage or current source inverters was used in the control of multiphase induction machines in the late sixties to the early nineties of the last century [1], [2], [3]. Currently, vector control and direct torque control (DTC) methods have taken center stage in research and applications since the cost of multiphase power electronics is higher compared to the cost of implementing control algorithms [4]. Both these methods rely on accurate mathematical models of the machine.

Theoretically, the same vector control schemes used in the control of three-phase induction machines are applicable to symmetrical multiphase machines regardless of the number of phases. Here, the co-ordinate transformation has to produce the required stator current or voltage references. Some applications of vector control of multiphase induction machine drives include [5], [6], [7]. Similarly, the same techniques for DTC of three-phase induction machines drives can be appropriately used in multiphase induction machines drives. DTC improves the operating characteristics of the motor and the voltage source inverter through the control of the stator flux and the torque, instead of controlling the current [8]. The DTC principle is based on instantaneous space vector theory. Simultaneous and decoupled control of torque and stator flux is achieved by optimal selection of space voltage vectors in each sampling period in accordance with the torque and flux errors. Then, the performance of a DTC scheme is directly affected by the number of space vectors and switching frequency. Results have shown that DTC of multiphase induction machine drives can achieve higher performance [9], [10], [11]. The vector control and DTC of a five-phase induction motor are compared in [12]. The authors showed that by utilizing current injection, vector control provides the desired nearly rectangular current and flux waveforms, and DTC results in a significant reduction of torque and stator current ripples. The complexity of the vector control and DTC algorithm increases as the number of phases increases [13].

Although the multiphase induction machine drive offers several attractive advantages over the conventional three-phase induction machine drive, it is restricted to highly specialized applications. One aspect of the multiphase induction machine drive is the complexity of the control algorithm for decoupled flux and torque control. The complexity, arising from the required coordinate transformations, increases with increase in the number of phases of the machine. To overcome the complexity problem, a method that allows the control of a six-phase induction machine drive without any coordinate transformations was developed and tested [14]. This new control technique allows the control of the machine to be similar to that of dc machines through the use of special trapezoidal-shaped stator current waveforms. These stator phase current waveforms consist of field (flux) and torque current components, with flat-topped amplitudes allowing a stator phase to act alternately in time as either a flux or a torque producing phase. The idea is to have a number of stator phases acting as flux producing phases, whilst the remaining phases act as torque producing phases at each time instance. In this paper, the description of the drive as a "direct flux and direct torque controlled" drive is avoided as "direct flux control (DFC)" and "direct torque control (DTC" are well-known control methods used in conventional induction machine drives. Instead, the type of drive proposed by [14] and considered in this paper is rather referred to as a "brush-dc equivalent" (BDCE) multiphase induction machine drive.

In this paper, the BDCE control concept, and the principle of operation of the so-called direct flux and direct torque control method for multiphase induction machine drives is explained. Also, a method that can be used to analytically calculate the air-gap flux density of a BDCE controlled machine is given. A comparison of analytically calculated and measured torque of the machine is also given.

II. DEVELOPMENT OF BDCE MACHINE CONCEPT

In salient dc machines, a compensating winding, as shown in Fig. 1, can be used to obtain a more uniform air-gap flux distribution and to mitigate the saturation effect due to the armature reaction flux. The compensating coils are mirror images of the armature coils and have the same number of ampere-turns as the armature. In practice, if the compensating coils have the same number of turns as the armature coils, they are connected in series with the armature coils. The function of the compensating coils is to cancel the flux produced by the armature coils, thus leaving only the flux produced by the field winding. Starting with Fig. 1, the dc machine can be transformed by replacing the salient stator with a round stator and shifting the phases as shown in Fig. 2. This type of dc machine should work similar to the one shown in Fig. 1. To

978-1-4673-4569-9/13/$31.00 ©2013 IEEE

realize a BDCE controlled induction machine, all the windings (field and compensating from Fig. 2) are placed in evenly spaced identical slots on a non-salient round stator and the number of turns is maintained the same in all the stator slots. The compensating (torque) windings are replaced with individual coils that become a group of torque phases and the field windings are replaced with independent coils that become a group of field phases as shown in Fig. 2. The armature winding is replaced with a cage (or wound rotor) winding.

For the induction machine to operate, carefully selected stator current waveforms, that have a field component that will produce a rotating air-gap MMF when applied to a particular stator winding layout, have to be realized. Trapezoidal stator current waveforms that produce a rectangular flux density in the air-gap were proposed in [14] for the control of a six phase induction machine. The waveform allows for the separate control of a field current- and a torque current-component which in turn leads to a simple control system (BDCE control). These phase current waveforms are made possible through the use of full-bridge converters per phase of the induction multiphase machine. The flux produced by the field producing phases leads to induced voltages at slip speed in the rotor bars located under the torque phases. Then, the rotor phase currents will flow in the cage or shorted wound rotor winding under the torque phases and produce a flux in quadrature to the main flux. The interaction between the rotating field and the rotor currents will produce torque in the machine. Note that the field generated by the rotor currents would distort the stator current produced field and thus reduce the electromagnetic torque. The torque current flowing in the torque phases must then produce a counter MMF to balance the MMF due to the rotor current similarly to the compensating winding in dc machines. Therefore, the stator current waveforms have to allow a phase to alternate between being a field producing phase and a torque producing phase. At each time instance, a group of phases are to act as field producing phases and the rest as torque producing phases. The stator waveforms when applied to a properly designed stator winding layout are to produce a moving rectangular air-gap flux density when the rotor MMF is cancelled by the MMF produced by the torque winding at each instance. Thus, torque in the machine is produced similarly as in dc machines with compensating windings.

A. *Constructing the Stator Current Waveforms*

In Fig. 3, a trapezoidal stator current waveform where the number of field phases, m_f, and the number of torque phases, m_t is shown. The sum of m_f and m_t gives the total number of stator phases for the machine, m. I_f and I_t are the amplitudes of the field and torque current respectively. For a machine with m stator phases, the phases are grouped into three groups with each group made of $m/3$ phases. The appropriate combination of mf and mt is selected using the algorithm in [15]. It can be seen from the waveform that m_f and m_t must be greater or equal to three, otherwise, the waveform shape will be lost. All the other phases are constructed by phase shifting this waveform by

$$\varphi = \frac{2\pi}{3}(z-1) + \frac{\pi}{m}(i-1), \qquad (1)$$

where φ is the phase shift, z = 1, 2, or 3 and i = 1, 2,…, $m/3$, z is the group index and i is the phase index. E.g the six phases shown in Fig. 4.

B. *Principle and Description of BDCE Multiphase Induction Machine Drive*

The basic principle of operation of the BDCE multiphase induction machine drive is explained using a six phase induction machine having stator phase current waveforms as shown in Fig. 4. In the figure, it is shown that the stator phase current consists of trapezoidal-shaped field and torque current components, with flat-topped amplitudes of I_f and I_t respectively. That is, a stator phase acts alternately in time as either a flux or a torque producing phase. Furthermore it can be seen from Fig. 4 and Fig. 5 that at any instant there are always three neighboring stator phase windings that act as field windings to generate the flux in the machine whilst the other three neighboring stator phase windings always act as torque windings to generate the torque of the machine. When the stator phase currents with the waveforms of Fig. 4 are applied to a stator the stator layout of Fig. 5, a separate rotating flux or field MMF with an amplitude, F_f, and torque MMF with an amplitude, F_t, will be produced in the two pole six-phase induction machine. The flux generated by the field winding in the machine will lead to induced rotor phase voltages at slip speed and currents will flow in the rotor phases. Then, the rotor currents produce the rotor MMF, F_r, which in turn affects the air-gap flux density. The torque MMF balances (cancels) the rotor MMF during operation of the BDCE multiphase induction machine ($F_t = F_r$ for balanced MMF condition (flux decoupling condition)) and the flux in the machine is only controlled through the field current. There is, thus, an important relationship between the torque current, I_t, and the angular slip frequency, ω_{sl}, for balanced MMF control (or decouple control), that is,

$$k = \frac{\omega_{sl}}{I_t}, \qquad (2)$$

where k is called the control gain. The relationship (2) is used in the control system of the drive.

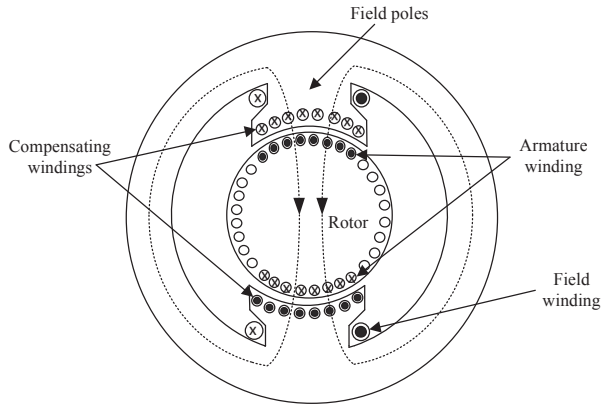

Fig. 1. Geometry of a brush dc machine with salient poles and pole-face compensating windings.

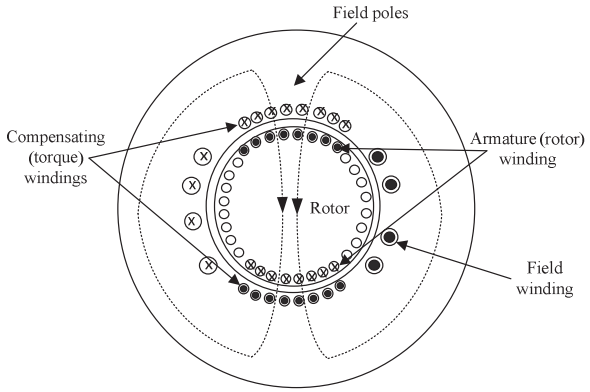

Fig. 2. Geometry of a non-salient round stator machine with compensating windings.

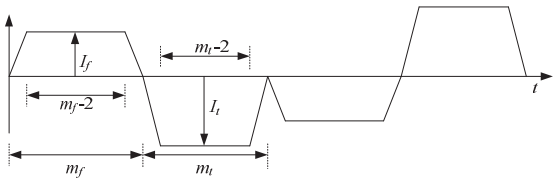

Fig. 3. Trapezoidal stator current waveform.

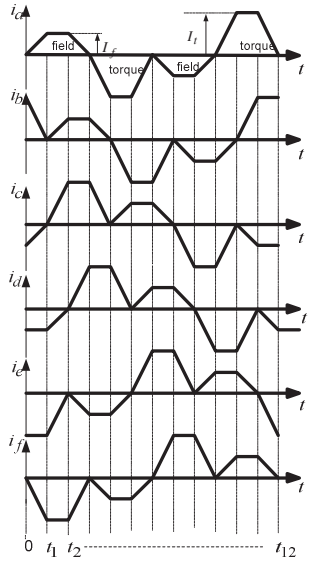

Fig. 4. Configuration of the trapezoidal six-phase current waveforms [14].

Fig. 6 shows a block diagram of an *m*-phase induction machine drive with its control system. Similarly to [16] and phase redundant multiphase systems [17], a full bridge inverter is used for each stator phase winding. The rotor speed together with the phase currents of the drive are measured and fed back to a digital signal processor (DSP) controller. The field current is kept constant and the torque command-current is controlled by the speed controller. The speed controller controls the torque command-current I_t from which the slip angular frequency ω_{sl} is determined using the control gain. From this and from the known field command current I_f, the *m* reference phase currents of the drive are generated. A digitally implemented hysteresis current regulator, using a field programmable gate array (FPGA), is used for the current

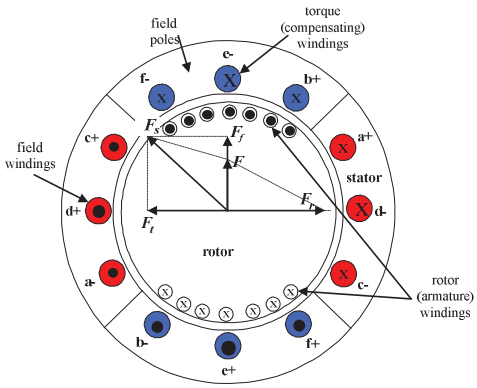

Fig. 5. Current distribution and MMF space phasors when α = 0.

control. The switching signals are sent to the inverter via fibre optic cables. Thus, the control method does not require any transformations.

C. Air-gap Flux Density

In order to perform analytical calculations, it is necessary to find a mathematical expression of the stator current waveforms. The Fourier transform can be applied on the waveform of phase *a* as follows,

$$i_a(t) = \sum_{n=-\infty}^{\infty} I(x) e^{jx\omega t} \tag{3}$$

where

$$I(x) = \frac{1}{T}\int_0^T i_a(t) e^{-jx\omega t} dt \tag{4}$$

and ω is the electrical angular frequency and x is the time harmonic order, x = 1, 2, 3… Therefore, the current waveform can be viewed to be made up of the addition of infinite independent sinusoidal waveforms of different frequencies. The higher the number of considered harmonics, the more accurately the waveform is estimated. Similarly, the mathematical representation of the other waveforms can be obtained as for $i_a(t)$.

The MMF waveform for a single coil with N turns and i current flowing in a four pole machine stator is shown in Fig. 7 , where F is the MMF and θ is in electrical radians. When infinite permeability in the iron is assumed, the MMF in the stator and rotor can be neglected and therefore the MMF across the air-gap is equal to the total MMF.

Thus, the Fourier transform for the MMF waveform of Fig. 7 is

$$F(\theta) = \sum_{m=-\infty}^{\infty} F(v) e^{jvp\theta} \tag{5}$$

$$F(v) = \frac{1}{\pi}\int_0^{\pi} F(\theta) e^{-jvp\theta} d\theta\,, \tag{6}$$

where, p is the number of pole pairs and v is the harmonic order. Applying integration by parts yields

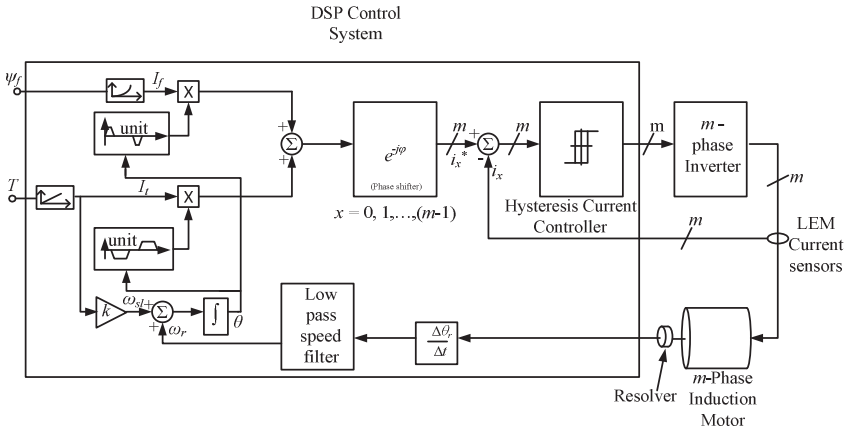

Fig. 6. BDCE control system operation.

$$F(v) = \frac{Ni}{4\pi v}\left(2je^{-jvp\pi} - j - je^{-2jvp\pi}\right). \quad (7)$$

And hence

$$F(\theta) = \sum_{v=1}^{\infty} \frac{2Ni}{\pi v}\sin(vp\theta)\, v = 1, 3,\ldots.. \quad (8)$$

The current, i, is considered to be an instantaneous current such as $i_a(t)$. Each of the m-phase stator current waveforms will produce a corresponding MMF derived similar to (8), differing only by a phase angle. Finally, the MMF due to the stator winding is found by summing the individual MMFs,

$$F_s(\theta) = \sum_{j=a}^{m} F_j(\theta). \quad (9)$$

Each stator current harmonic contribution to the total MMF can be evaluated independently. Assuming infinite permeability of iron, the air-gap flux density, $B(\theta)$, can be expressed in terms of the MMF calculated given in equation (8) as,

$$B(\theta) = \frac{\mu_0 F_s(\theta)}{2g} \quad (10)$$

where, g is the air-gap length, μ_o is absolute permeability.

D. Static torque of the machine

The method of evaluating the air-gap flux density described in this section is an extension of the method introduced by [14] and described in [18]. Using the method described in [15], the air-gap flux density versus field current relationship is obtained for the m-phase machine. From this relationship, the air-gap flux density and the field current values are obtained. The square like shaped air-gap flux density leads to a square like induced voltage waveform in the rotor bar [14] [18].The dc flat-topped induced rotor bar current is then given by

$$I_r = \frac{E_b}{R_b} = \frac{2N_r Bl\omega_{sl} r_g}{R_r}, \quad (11)$$

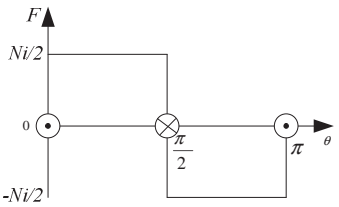

Fig. 7. MMF waveform produced by a full-pitch single coil for a four pole induction machine.

where, E_b is flat-topped amplitude of the induced bar voltage, R_b is the dc bar resistance, N_r is the number of turns per rotor phase (N_r = 0.5 for a squirrel cage winding), B is the air-gap flux density, l is the stack length, ω_{sl} is angular slip frequency and r_g is the air-gap radius. The bar inductance is neglected (the end ring resistance is ignored in this analytical calculation).

The torque of the machine can be calculated by using the Lorentz force law and is given by

$$T = 4pm_{ra}N_r BI_r lr_g, \quad (12)$$

where m_{ra} is the number of active bars per pole. Assuming MMF balance between the torque MMF and the rotor MMF ($F_r = F_t$), as this is a requirement for the operation and control of the machine using BDCE control, it can be shown that the amplitude of the stator torque MMF produced by the m_t torque phase winding at any instant, is

$$F_t = \frac{(m_t - 1)N_s I_t}{2p}, \quad (13)$$

where, N_s is the number of series turns per stator phase. The amplitude of the rotor air-gap MMF is given by

$$F_r = m_{ra}N_r I_r. \quad (14)$$

Then, the stator torque current is calculated with $F_r = F_t$ and is given by

$$I_t = \frac{2pm_{ra}N_r I_r}{(m_t - 1)N_s}. \quad (15)$$

The relationship between I_t and w_{sl} is therefore given by

$$k = \frac{w_{sl}}{I_t} = \frac{(m_t - 1)N_s R_r}{4pm_{ra}N_r^2 Blr_g}. \quad (16)$$

Since the value of k is dependent on the bar resistance, which in turn is dependent on temperature, a machine designer must know the operational temperature of the machine precisely before calculating the value of k. B can be controlled through the field current, I_f. From equations (12) and (15), the torque can also be expressed as,

$$T = 2(m_t - 1)N_s I_t Blr_g. \quad (17)$$

Hence, under balanced MMF conditions, the electromagnetic torque is directly proportional to the torque current as observed in dc machines.

III. Practical Considerations

A standard 11 kW, four-pole, 36-slot, three-phase induction machine stator is rewinded to a nine-phase stator with full-pitch (concentrated) coils. The parameters of the machine are given in Table 1.The nine-phase inverter comprises of Intelligent Power Modules (IPMs), the control and isolated power circuits, the dc bus bar and per phase current sensors. Modular design is utilized in the design of the inverter since it allows for independent testing and simple replacement of faulty boards. An H-bridge is required for each phase of the nine-phase machine, thus, the inverter consists of six 6MBP25RA120 three-phase intelligent power modules (IPMs). Each control board is shared by two IPMs. Based on the method presented in [15], the optimal (best) ratio of the number of field phases to torque phases,

$$m = \frac{m_f}{m_t}, \quad (18)$$

is calculated for the 9-phase machine as $m = 0.5$ (that is, $m_f = 3$ and $m_t = 6$).

IV. Results

Air-gap flux density waveforms of a BDCE controlled four-pole, 36-slot, nine-phase induction machine with full-pitch (concentrated) coils are given in this section. Under BDCE control, the field in the air-gap is produced by the field current. Then, the air-gap flux density of the machine is calculated with I_t = 0 A, I_f = 5.83 A and the rotor currents equal zero. The flux density calculated from the MMF at a stationary point on the air-gap with the machine excited by the trapezoidal current waveforms at locked rotor, is shown Fig. 8 . The analytically calculated air-gap flux density has flat topped amplitude of 0.63 T. Also, the analytically calculated air-gap flux density around the air-gap at a particular time instance is shown in Fig. 9. The FEA (JMAG) calculated flux density is shown in Fig. 10 with visible slotting effects. The average air-gap flux density calculated through FEA has average amplitude of 0.71 T. There is agreement between the analytical results, Fig. 9, and the FEA results, Fig. 10, with the latter showing visible slotting effects since an un-skewed rotor is considered. An FEA calculated field plot of the machine is shown in Fig. 11.

Table 2 gives the comparison of the finite element analysis (FEA), analytically calculated and measured torque values at rated conditions. From the table, it is clear that the analytical method provide a good approximation of the torque in the machine. The effects of changing k values are evaluated through measurements as shown in Fig. 12. The figure shows that a wrong value of k leads to the loss of the linear relationship between torque and torque current, that is, the loss of the MMF balance in the machine.

I. Conclusions

The BDCE control concept is presented in this paper. An expression for evaluating the air-gap flux density is developed. From the balanced MMF condition assumption, an analytical expression of the static torque of the machine is derived through the application of Lorentz force law. Both analytical and theoretical results show that there is a moving square-like air-gap flux density in the air gap similar to that of dc machines. The sensitivity of the control method to varying control gain (k) values is shown through practical measurements of the torque versus current. The results show that a wrong value of k can lead to the loss of MMF balance in the machine. The BDCE control method is simpler than coordinate transformation based control schemes such as vector control. It is suitable for large multiphase induction machine drives.

TABLE 1. PARAMETERS OF A 4-POLE 9-PHASE INDUCTION MACHINE

Rated Power, P_n	11kW
Air-gap length, g	0.5 mm
Stack length, l	127 mm (copper
Rotor radius	84.5 mm
End ring segment resistance, R_e	1.28e-6 Ω (75°C)
End ring segment inductance, L_{er}	29.2 nH
Number of field phases, m_f	3
Number of torque phases, m_t	6
Number of rotor bars, M_r	28
Number of stator slots, M_s	36
Number of series turns per stator phase, N_s	170
Torque current, I_t	5.5 A
Field current, I_f	5.83 A
Bar height	25 mm
Bar width	4.5mm
Operating speed	1466 r/min

TABLE 2. RATED TORQUE WITH I_f = 5.83 A, I_t = 5.5 A AND k = 0.638 AT A ROTOR SPEED OF 1466 R/MIN

	Torque (Nm)
FEA	67.5
From equation (17)	70.4
Measured	67

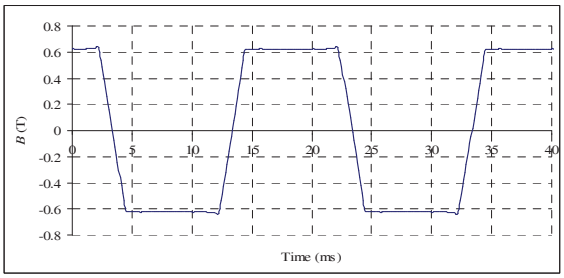

Fig. 8. Calculated flux density in the air-gap at a stationary point (x = 1, 3…, 49, v = 1, 3…, 99).

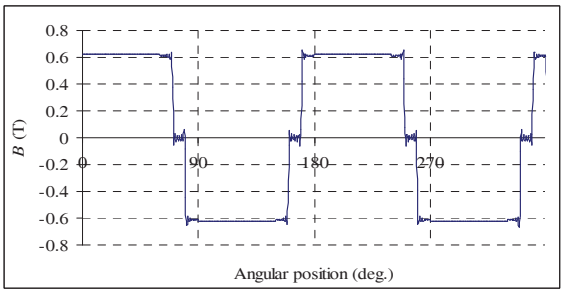

Fig. 9. Calculated flux density in the air-gap around the induction machine (x = 1, 3…, 49, v = 1, 3…, 99).

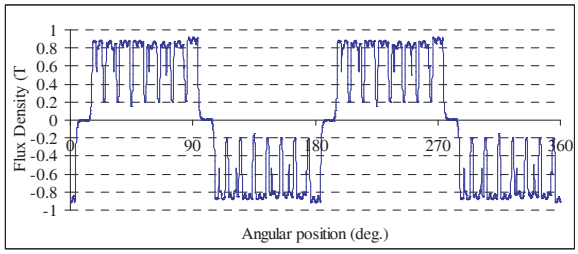

Fig. 10. FEA air-gap flux density for the induction machine at time t = 0.

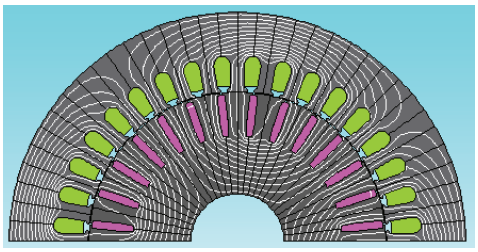

Fig. 11. FEA (JMAG) calculated field plot of the nine-phase four pole induction machine..

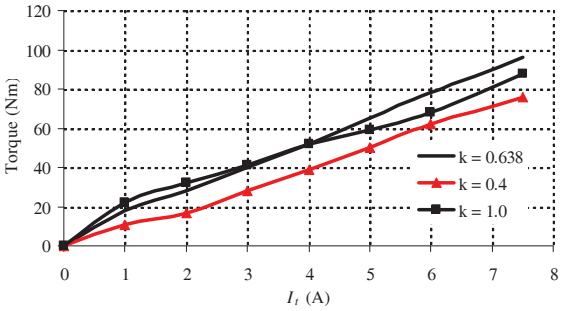

Fig. 12. Measured effect of different k-values at 500 r/min.

REFERENCES

[1] E. E. Ward and H. Harer, "Preliminary investigation of an invertor-fed 5-phase induction motor," Proceedings of IEE, vol. 116, pp. 980-984, 1969.

[2] K. N. Pavithran, R. Parimelalagan, and M. R. Krishnamurthy, "Studies on Inverter-Fed Five-Phase Induction Motor Drive," IEEE Transactions on Power Electronics, vol. 3, pp. 224-235, 1988.

[3] K. Gopakumar, S. Sathiakumar, S. K. Biswas, and J. Vithayathi, "Modified current source inverter fed induction motor drive with reduced torque pulsations," IEE Proceedings Electric Power Applications Part B, vol. 131, pp. 159 - 164, 1984.

[4] E. Levi, "Multiphase electric machines for variable-speed applications," IEEE Transactions on Industrial Electronics, vol. 55, pp. 1893-1909, May 2008 2008.

[5] R. Bojoi, G. Griva, and F. Profumo, "Field Oriented Control of Dual Three-Phase Induction Motor Drives using a Luenberger Flux Observer," in 41st Industry Applications Conference Annual Meeting, 2006.

[6] S. N. Vukosavic, M. Jones, E. Levi, and J. Varga, "Rotor flux oriented control of a symmetrical six-phase induction machine," Elsevier Electric Power Systems Research, vol. 75, pp. 142-152, 2005.

[7] A. D. Graham, "Vector control of a multiphase induction motor with open circuit phases," in IEEE International Electric Machines and Drives Conference, IEMDC '09, 2009.

[8] S. Mythili and K. Thyagarajah, "Direct Torque Control (DTC) of Multi-phase Induction Motor using TMS320F2407 Digital Signal Processor," in International Conference on Power Electronics and Drives Systems, PEDS 2005, 2005, pp. 1024 - 1029.

[9] R. Kianinezhad, R. Alcharea, B. Nahid, F. Betin, and G. Capolino, "A novel direct torque control (DTC) for six-phase induction motors with common neutrals," in International Symposium on Power Electronics, Electrical Drives, Automation and Motion, SPEEDAM 2008, 2008, pp. 107 - 112.

[10] R. Bojoi, F. Farina, G. Griva, F. Profumo, and A. Tenconi, "Direct Torque Control for Dual Three-Phase Induction Motor Drives," IEEE Transactions on Industry Applications, vol. 41, pp. 1627-1636, 2005.

[11] K. Hatua and V. T. Ranganathan, "Direct Torque Control Schemes for Split-Phase Induction Machine," IEEE Transactions on Industry Applications, vol. 41, pp. 1243-1254, 2005.

[12] X. Huangsheng, H. A. Toliyat, and L. J. Petersen, "Five-phase induction motor drives with DSP-based control system," IEEE Transactions on Power Electronics, vol. 17, pp. 524 - 533, 2002.

[13] E. Levi, R. Bojoi, F. Profumo, H. A. Toliyat, and S. Williamson, "Multiphase Induction Motor Drives - A Technology Status Review," IEE Proceedings - Electric Power Applications, vol. 1, pp. 489-516, July 2007.

[14] Y. Ai, M. J. Kamper, and A. D. L. Roux, "Novel Direct Flux and Direct Torque Control of Six-Phase Induction Machine with Nearly Square Air Gap Flux Density," IEEE Transactions on Industry Applications, vol. 43, pp. 1534-1543, December 2007.

[15] N. Gule and M. J. Kamper, "Optimal Ratio of Field to Torque Phases in Multi-Phase Induction Machines Using Special Phase Current Waveforms," in Proceedings of International Conference on Electrical Machines (ICEM2008), 2008.

[16] L. Weichao, H. An, G. Shiguang, and S. Chi, "Rapid Control Prototyping of Fifteen-Phase Induction Motor Drives Based on dSPACE," in International Conference on Electrical Machines and Systems, ICEMS 2008, 2008.

[17] G. K. Singh, "Multi-Phase Induction Machine Drive Research - A survey," Elsevier Electric Power Systems Research, pp. 139-147, 2002.

[18] N. Gule and M. J. Kamper, "Multi-phase Cage Rotor Induction Machine with Direct Implementation of Brush DC Operation," in International Electric Machines and Drives Conference (IEMDC2011) Niagara Falls, Canada, 2011.